Materials and Methods

Cell lines

The mouse B cell line BAL17 and its transfectants were cultured in RPMI 1640 medium supplemented with 10% FCS, 50 μM 2-ME, 1 mM L-glutamine, and 100 U penicillin/streptomycin. The retrovirus packaging cell line PLAT-E (a gift of Dr. T. Kitamura, University of Tokyo, Tokyo, Japan) (23) was maintained in DMEM supplemented with 10% FCS, 2 mM L-glutamine, and 100 U penicillin/streptomycin. Embryonic stem (ES) cell line R-CMTI-2A derived from B6 mice was purchased from Dainippon Sumitomo Pharma (Osaka, Japan) and was cultured in DMEM medium supplemented with 15% FBS, L-glutamine, nonessential amino acids, and LIF (Chemicon International).

Vector and retrovirus

The $CD72^a$ and $CD72^c$ cDNA was obtained from total RNA prepared from a DBA/2 and MRL/lpr mouse spleen, respectively, by RT-PCR using a set of primers (5′-CCGAATTCATGGCTGACGCTATCACG-3′ and 5′-AAGCGGCCGCTATATCCGGTTCAGTTCAG-3′). These fragments were inserted into the retroviral vector pMX (a gift of Dr. T. Kitamura) (24). For retrovirus production, the packaging cells were transfected with retroviral vectors using a calcium phosphate method. Cells were cultured for 48 h, and the culture supernatant was collected. BAL17 cells were incubated with the supernatant containing retrovirus in the presence of 5 μg/ml polybrene for 4 h.

Mice

B6 and MRL/lpr mice were purchased from Sankyo Laboratory Service (Tokyo, Japan). B6/lpr mice were purchased from Japan SLC (Hamamatsu, Japan). QM mice were as described previously (25) (a kind gift from Dr. M. Wabl, University of California, San Francisco, San Francisco, CA). To generate CD72-dificient mice, genomic DNA fragments containing *Cd72* were isolated by PCR from the bacterial artificial chromosome (BAC) clone derived from a B6 mouse. The targeting vector was constructed by inserting the neomycin resistance gene flanked by the *loxP* sequences upstream of the first exon of *Cd72* (Supplemental Fig. 2A). The linearized targeting vector was transfected by electroporation into the R-CMTI-2A ES cells. The $Cd72^{+/-}$ ES cell clones 4 and 150 (Supplemental Fig. 2B) were used for blastocyst injection to generate chimeric mice. Lack of CD72 expression in $Cd72^{-/-}$ mice was confirmed by flow cytometry and Western blotting (Supplemental Fig. 2C, 2D). All mice used in this study were bred and maintained in a specific pathogen-free animal facility of Tokyo Medical and Dental University and handled according to our institutional guidelines.

Genotyping

Genomic DNA was extracted from mouse tail and genotyping was done by PCR. Microsatellite primers *D4Mit268*, *D4Mit193*, *D4Mit196*, *D4Mit91*, *D4Mit241*, *D4Mit17*, *D4Mit9*, *D4Mit308*, and *D4Mit203*, located at 8.73, 13.99, 20.16, 23.04, 30.48, 33.96, 43.34, 57.66, and 63.26 cM distal from the centromere on chromosome 4, respectively, were synthesized according to Mouse Genome Informatics (The Jackson Laboratory). The $Cd72^b$ and $Cd72^c$ allele were specifically amplified using the following primers sets: $Cd72^b$ forward, 5′-ACATATTACCAGAAGTGGGA-3′ and reverse, 5′-GGTTAAGGATGTAGGTCACAAGGTCTT-3′; and $Cd72^c$ forward, 5′-ATATATAACAAGAAGTGGGC-3′ and reverse, 5′-GGTTAAGGATGTAGGTCACAAGGTCTT-3′. Fas^{WT} and Fas^{lpr} were specifically amplified using the following primers: forward primer, 5′-TTTACTCATTGACTTATCAAGT-3′; reverse primer specific for Fas^{WT}, 5′-AGCCTCCAGGGCCTTCACCTTCTCA-3′; and a reverse primer specific for Fas^{lpr}, 5′-CAAATTTTATTGTTGCGAC-3′.

Flow cytometry analysis

Single-cell suspensions were prepared and stained with the following Abs: FITC-conjugated anti-CD3ε mAb (145-2C11), PE-conjugated anti-CD5 mAb (53-7.3), FITC-conjugated anti-CD21 mAb (7E9) (BioLegend); PE-conjugated anti-CD23 mAb (B3B4), PE-conjugated anti-$CD72^{b+c}$ mAb (JY/93; BD Pharmingen); FITC-conjugated anti-$CD72^{a+b}$ mAb (K10.6; a kind gift from Dr. N. Tada, Tokai University, Tokyo, Japan) (26), Alexa Fluor 647–labeled anti-B220 Ab (RA3-6B2), PE-conjugated anti-CD138 mAb (c363.16A; eBioscience), and FITC-conjugated goat anti-mouse IgM (Southern Biotechnology Associates). Data was collected by a FACSCalibur (BD Biosciences) or a CyAn ADP (DakoCytomation) and analyzed using the FlowJo software (Tree Star) or Summit software (DakoCytomation), respectively.

ELISAs

Serum levels of total IgG were measured by standard sandwich ELISA. Titers of IgG Ab to dsDNA, ssDNA, and chromatin were measured by ELISAs as described previously (27). Briefly, ELISA plates were coated with 10 μg/ml dsDNA, 10 μg/ml ssDNA, or 4 μg/ml chromatin. After blocking with 0.5% BSA in PBS, 50 μl diluted serum samples were added and incubated for 60 min at room temperature. Plates were then washed and incubated with alkaline phosphatase–conjugated goat anti-mouse IgG Ab (Southern Biotechnology Associates). After washing, plates were reacted by phosphatase substrate (Sigma-Aldrich), and the absorbance at 405 nm was measured on a Vmax kinetic microplate reader (Molecular Devices). Autoantibody titers were determined using the sera pooled from (NZB × NZW) F1 mice >8 mo old as a standard.

Immunoprecipitation and Western blotting

B cells were purified from mouse spleen as described previously (28) and were stimulated with 0.2 μg/ml 4-hydroxy-3-nitrophenyl acetyl (NP)-BSA or 10 μg/ml $F(ab')_2$ fragments of goat anti-mouse IgM Ab (Jackson ImmunoResearch Laboratories). Alternatively, BAL17 cells were stimulated with 10 μg/ml $F(ab')_2$ fragments of goat anti-mouse IgM Ab at 37°C. Cells were lysed in Triton X-100 lysis buffer (1% Triton X-100, 10% glycerol, 150 mM sodium chloride, 20 mM Tris-HCl, 2 mM EDTA, 0.02% sodium azide, 10 μg/ml PMSF, and 1 mM sodium orthovanadate) and immunoprecipitated with rat anti-CD72 mAb JY/93 (BD Pharmingen) using protein G-Sepharose (Amersham Biosciences). Total cell lysates or immunoprecipitates were separated by SDS-PAGE and transferred to polyvinylidene difluoride membranes (Millipore). Membranes were incubated with goat anti-mouse IgM Ab (Southern Biotechnology Associates), rabbit anti-CD72 Ab (Santa Cruz Biotechology), or rabbit anti-p42/44 ERK Ab (Cell Signaling Technology), followed by reaction with HRP-conjugated donkey anti-goat IgG Ab (Santa Cruz Biotechnology) or HRP-conjugated goat anti-rabbit IgG Ab (Southern Biotechology Associates). Alternatively membranes were incubated with mouse anti–β-tubulin Ab TUB2.1 (Seikagaku Kogyo), followed by reaction with HRP-conjugated goat anti-mouse IgG Ab (Southern Biotechology Associates). Proteins were then visualized using ECL system (Amersham Biosciences). The intensity of protein bands was quantified using the Image J software (National Institutes of Health).

Measurement of intracellular calcium concentration

Spleen B cells were purified as described previously (29). BAL17 cells and its transfectants or purified spleen B cells (1×10^6) were incubated in culture medium containing 5 μg Fluo-4/AM (Molecular Probes) at 37°C for 30 min. Cells were stimulated with 10 μg/ml $F(ab')_2$ fragments of anti-IgM Ab or 0.2 μg/ml NP-BSA, and fluorescence was continuously measured by an FACSCalibur (BD Bioscience) for a total of 300 s.

Measurement of cell proliferation by CFSE dilution

Spleen B cells were purified as described previously (28) and labeled with 5 μM CFSE (Molecular Probes). The purity of purified cells was determined by flow cytometry using anti-B220 Ab staining (purity >93%). Cells (2×10^5/ well) were then seeded into 96-well plate and cultured in RPMI 1640 medium supplemented with 10% FCS, 50 μM 2-ME, 1 mM L-glutamine, and 100 U penicillin/streptomycin with or without 10 μg/ml anti-CD40 Ab (FGK45) (30), 10 μg/ml $F(ab')_2$ fragment of goat anti-mouse IgM Ab (Jackson ImmunoResearch Laboratories), or 10 ng/ml CpG oligomer (ODN 1668) (31) at 37°C for 72 h. The fluorescence of CFSE was measured by a CyAn ADP (DakoCytomation).

Histopathological and immunohistochemical analysis

Mice were sacrificed, and tissues were fixed in neutral buffered formalin and embedded in paraffin according to standard practices. Tissue sections (5 μm) were stained with either H&E or periodic acid–Schiff and hematoxylin (PASH). Glomerular damages were scored as described previously (32). For immunohistochemical analysis, portions of kidney were embedded in Tissue-Tek OCT compound (Sakura) and snap frozen in liquid nitrogen. Cryostat sections (7-μm thickness) were mounted onto slide glass. The sections were incubated with blocking buffer (PBS containing 0.5% BSA and 0.05% sodium azide) for 30 min and stained with FITC-conjugated anti-mouse IgG Ab (Cappel) or FITC-conjugated anti-mouse C3 Ab (Cappel) at room temperature for 1 h. Sections were analyzed using a laser-scanning microscope Leica DMI6000B (Leica Microsystems).

Detection of proteinuria

The protein level of mouse urine was semiquantitatively analyzed as described previously (33).

Statistical analysis

The data are presented as the means ± SEM, and all statistical analyses were performed using GraphPad Prism 5.0 software (GraphPad). The p values were calculated with the two-tailed Student t test ($*p < 0.05$, $**p < 0.01$, $***p < 0.001$).

Results

Spontaneous development of lupus-like disease in B6.CD72^c/lpr congenic mice

B6/lpr and C3H /lpr mice are reported to show no or only a mild autoimmune disease (8, 9), whereas AKR/lpr and MRL/lpr mice develop moderate and severe lupus-like disease, respectively, suggesting that some genes carried by AKR and MRL mice are required for *Fas*^{lpr}-induced autoimmune disease. To address whether such a gene is located in the *Cd72*^{c} locus carried by both AKR and MRL, we generated B6.CD72^c congenic mice carrying the MRL-derived *Cd72*^{c} haplotype by selective backcrossing of the F1 hybrid between B6 carrying *Cd72*^{b} and MRL mice to B6 mice for 11 generations. Microsatellite marker analysis revealed that B6.CD72^c mice carry an MRL/lpr-derived interval on chromosome 4 containing the *Cd72*^{c} locus (Supplemental Fig. 1A). We then generated B6.CD72^c/lpr mice by crossing B6.CD72^c mice with B6/lpr mice. B6.CD72^c/lpr mice at 12 mo of age showed marked splenomegaly (Fig. 1A) and moderate lymphadenopathy (data not shown) compared with B6/lpr mice, whereas the spleen weight in B6.CD72^c mice was similar to that in B6 mice. Flow cytometry analysis revealed that percentages of T cells and B cells in both spleen and lymph nodes (LNs) of B6.CD72^c mice were

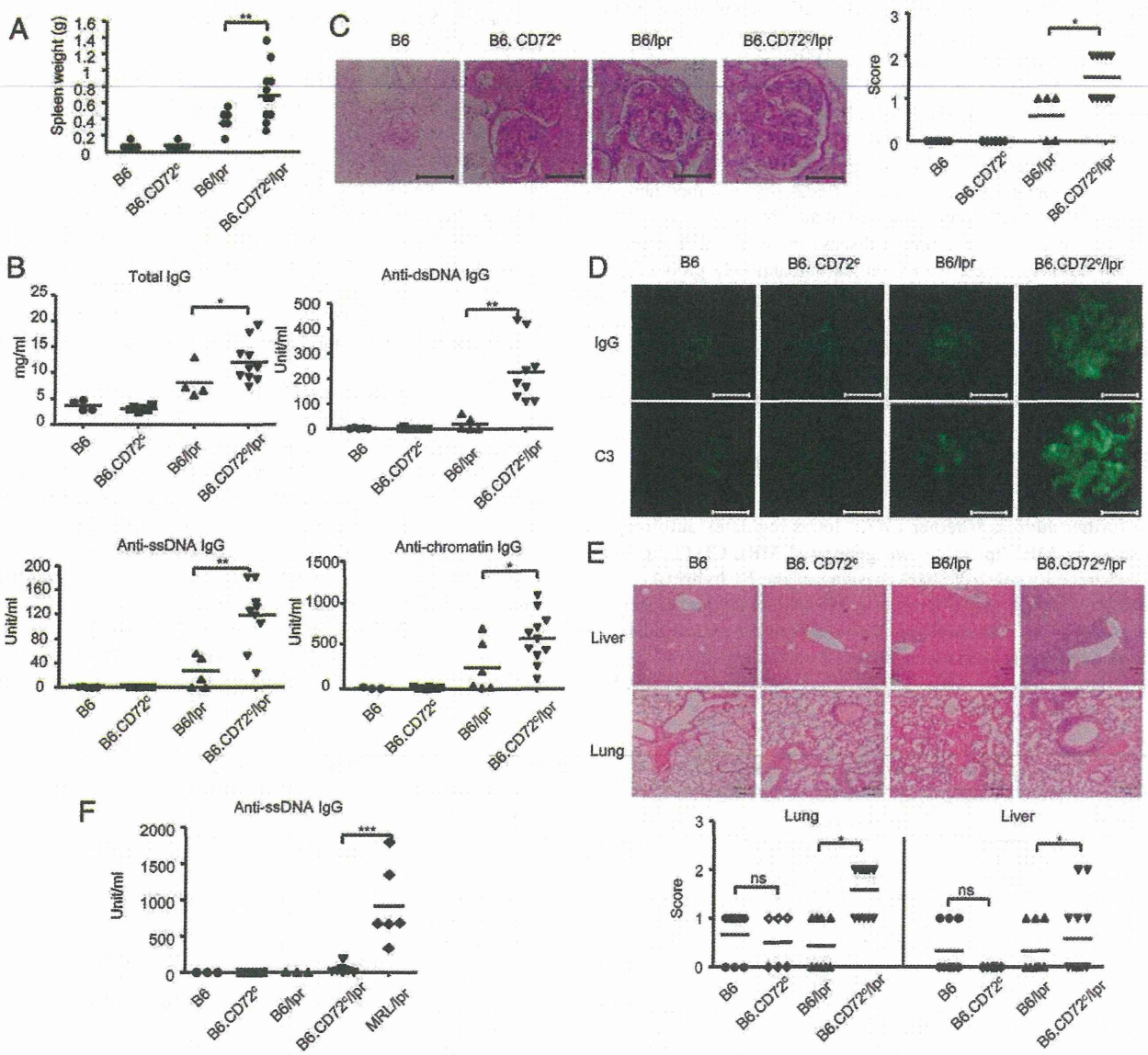

FIGURE 1. Lupus-like disease in B6.CD72^c /lpr congenic mice. (**A–E**) One-year-old female B6, B6.CD72^c, B6/lpr, and B6.CD72^c/lpr mice (n = 6–11) were analyzed. (A) Spleen weight. (B) Concentrations of total IgG and titers of indicated autoantibodies in sera. Horizontal bars represent mean values. For determining autoantibody titers, pooled sera from >8-mo-old (NZB × NZW) F1 mice are used as a standard (1000 U/ml). (C) PASH staining of glomeruli. Severity of glomerular damage was scored as described previously (32). Grade 0, no involvement; grades 1, 2, and 3, changes in 0–25%, 25–50%, and 50–75% of total glomeruli, respectively; grade 4, sclerosis or crescent formation in >90% of glomeruli. Scale bars, 50 μM. (D) Immunohistochemical analyses for IgG and C3 in glomeruli. Scale bars, 50 μM. (E) H&E staining of liver and lung. Representative data of more than five mice in each genotype are shown (original magnification ×100). Severity of the disease was scored according to the degree of lymphocyte infiltration. Grade 0, no lymphocyte infiltration; grade 1, moderate lymphocyte infiltration; and grade 2, severe lymphocyte infiltration. (**F**) Serum titer of anti-ssDNA IgG. Six-month-old female B6, B6.CD72^c, B6/lpr, B6.CD72^c/lpr, and MRL/lpr mice were analyzed (n = 3–10). $*p < 0.05$, $**p < 0.005$, $***p < 0.001$.

similar to those of B6 mice (Table I). In contrast, B6.CD72^c/lpr mice showed marked reduction in the percentage of B cells and increase in the percentage of T cells compared with B6/lpr mice. The percentage of B220$^+$CD3$^+$ lpr T cells in B6.CD72^c/lpr mice was not increased compared with B6/lpr mice. Thus, introduction of the interval of chromosome 4 containing *Cd72*^{c} locus induced marked splenomegaly and altered T cell to B cell ratio in B6/lpr but not B6 mice, suggesting that the chromosomal interval containing *Cd72*^{c} locus does not modulate immune homeostasis by itself, but does so in the presence of *Fas*^{lpr} mutation.

Next we examined development of autoimmune disease in B6.CD72^c/lpr mice. Sera from 12-mo-old B6.CD72^c/lpr mice contained a much larger amount of IgG autoantibodies such as anti-dsDNA, anti-ssDNA, and anti-chromatin Abs compared with B6/lpr mice (Fig. 1B). Histopathological and immunohistological analysis of kidney revealed that B6.CD72^c/lpr mice developed more severe glomerular lesions with more prominent immune complex deposition compared with B6/lpr mice (Fig. 1C, 1D). Moreover, B6.CD72^c/lpr mice showed severe cell infiltration in lung and liver, whereas cell infiltration in these organs was mild in B6/lpr mice (Fig. 1E). In contrast, B6.CD72^c mice did not show any pathological findings including kidney, lung, and liver. Thus, the chromosomal interval containing *Cd72*^{c} carries a modifier gene that regulates *Fas*^{lpr}-induced autoimmune disease.

To compare the autoimmune disease in B6.CD72^c/lpr mice to that in MRL/lpr mice, we examined autoantibody production in 6-mo-old B6.CD72^c/lpr mice and MRL/lpr mice because MRL/lpr mice do not survive until 12 mo old. The titer of serum anti-DNA IgG in B6.CD72^c/lpr mice was significantly lower than that in MRL/lpr mice (Fig. 1F). Thus, MRL loci other than the *Cd72*^{c} locus are also involved in the development of severe autoimmune disease in MLR/lpr mice.

Reduced severity in autoimmune disease in MRL.CD72^b/lpr congenic mice

To further address whether *Cd72*^{c} locus regulates autoimmune disease in MRL/lpr mice, we generated MRL.CD72^b/lpr congenic mice by selective backcrossing of the F1 hybrid between MRL/lpr and B6 (*Cd72*^{b}) mice to MRL/lpr mice for 12 generations. Analysis with microsatellite markers demonstrated that a B6-derived interval on chromosome 4 containing the *Cd72* locus was introduced into MRL.CD72^b/lpr mice (Supplemental Fig. 1B). We analyzed 6-mo-old female MRL.CD72^b/lpr mice and age-matched female MRL/lpr mice. Compared to MRL/lpr mice, spleen weight (Fig. 2A), the percentage of lpr T cells in spleen (Fig. 2B), and the serum titer of anti-dsDNA and anti-ssDNA IgG (Fig. 2C) were markedly reduced in MRL.CD72^b/lpr mice. Although histological score on renal disease based on the percentage of the affected glomeruli was not much improved in MRL.CD72^b/lpr mice (Fig. 2D), these mice showed smaller glomerular size (Fig. 2E), reduced immune complex deposition (Fig. 2F), and reduced urine protein level (Fig. 2G), suggesting improvement of renal disease in MRL/lpr mice by replacing the chromosomal interval including *Cd72* locus by the B6-derived interval. Taken together, the chromosomal interval including *Cd72*^{c} plays a role in development of autoimmune disease in MRL/lpr mice, especially in expansion of lpr T cells and autoantibody production.

Augmented BCR signaling and B cell proliferation in B cells carrying CD72^c

To elucidate whether CD72^c is functionally distinct from CD72^b, we crossed B6.CD72^c mice with the QM mice on a B6 background expressing CD72^b to generate QM. CD72^c mice. As almost all B cells from QM mice express BCR reactive to hapten NP due to their expression of knocked-in VH17.2.25 and λ L chain (25), we ligated BCR in spleen B cells from QM mice and QM. CD72^c mice using an Ag NP-conjugated BSA and examined BCR signaling by analyzing calcium mobilization and phosphorylation of ERK. Although the Ca^{2+} response in QM.CD72^c B cells was similar to that in QM B cells (Fig. 3A), QM.CD72^c B cells showed augmented ERK phosphorylation compared with QM B cells (Fig. 3B).

Next, we addressed proliferative response of *Cd72*^{c}-carrying B cells to various stimuli by CFSE dilution assay. When purified spleen B cells from B6 and B6.CD72^c mice were stimulated with CpG oligomers or anti-CD40 Ab, percentage of proliferated cells were significantly higher in B6.CD72^c cells than in B6 B cells (Fig. 3C). Percentage of divided cells after anti-IgM stimulation was not increased in B6.CD72^c B cells compared with B6 B cells probably because B6 B cells fully proliferated to this stimulation. Thus, Ag-induced ERK activation and proliferative response to CpG and anti-CD40 Ab were augmented in B6.CD72^c B cells, suggesting that CD72^c negatively regulates B cell activation less efficiently than CD72^b does, although the possibility that the other

Table I. Flow cytometry analysis of spleen and LN cells from B6, B6.CD72^c, B6/lpr, and B6.CD72^c/lpr mice

Tissue	Cell Population	B6	B6.CD72^c	B6/lpr	B6.CD72^c/lpr
Spleen	Total cell number ($\times 10^6$)	145.0 ± 11.0	127.0 ± 9.2	320.0 ± 100.0	764.3 ± 38.9*
	Phenotype (%)[a]				
	B220$^+$CD3$^-$ (B cells)	55.9 ± 3.1	56.0 ± 6.9	46.4 ± 3.9	18.1 ± 5.8**
	($\times 10^6$)[b]	(80.1 ± 4.8)	(69.2 ± 11.9)	(133.4 ± 38.3)	(137.6 ± 47.6)
	CD3$^+$B220$^-$ (T cells)	25.5 ± 3.2	20.3 ± 6.3	24.3 ± 3.4	40.5 ± 4.5*
	($\times 10^6$)	(37.9 ± 6.4)	(24.3 ± 9.9)	(89.2 ± 35.4)	(315.8 ± 43.4)**
	B220$^-$CD3$^-$	16.8 ± 1.9	21.4 ± 8.1	22.5 ± 4.4	34.5 ± 10.1*
	($\times 10^6$)	(25.3 ± 4.6)	(27.6 ± 9.6)	(84.0 ± 30.9)	(255.4 ± 75.8)**
	B220$^+$CD3$^+$ (lpr T cells)	1.6 ± 0.1	1.2 ± 0.4	6.7 ± 2.3	7.3 ± 2.7
	($\times 10^6$)	(3.4 ± 1.3)	(1.6 ± 0.6)	(13.4 ± 3.7)	(55.5 ± 21.2)*
LN	Phenotype (%)[b]				
	B220$^+$CD3$^-$ (B cells)	52.9 ± 6.3	44.2 ± 6.9	43.3 ± 3.0	17.9 ± 7.5*
	CD3$^+$B220$^-$ (T cells)	40.2 ± 6.3	45.1 ± 9.9	24.7 ± 4.1	52.0 ± 8.2*
	B220$^-$CD3$^-$	5.8 ± 1.1	9.4 ± 3.7	4.1 ± 2.6	1.9 ± 0.5
	B220$^+$CD3$^+$ (lpr T cells)	0.9 ± 0.2	1.1 ± 0.3	27.1 ± 1.3	27.3 ± 3.0

Data were obtained from 12–14-mo-old mice and are expressed as mean ± SEM (n = 6 to 7).

[a]Percentages of cells expressing the indicated surface markers in total lymphocyte-gated cells from spleen and LN.

[b]Absolute cell numbers are indicated in parentheses. Statistical significance was calculated between B6 and B6.CD72^c mice and between B6/lpr and B6/lpr.CD72^c mice.

*$p < 0.05$, **$p < 0.01$.

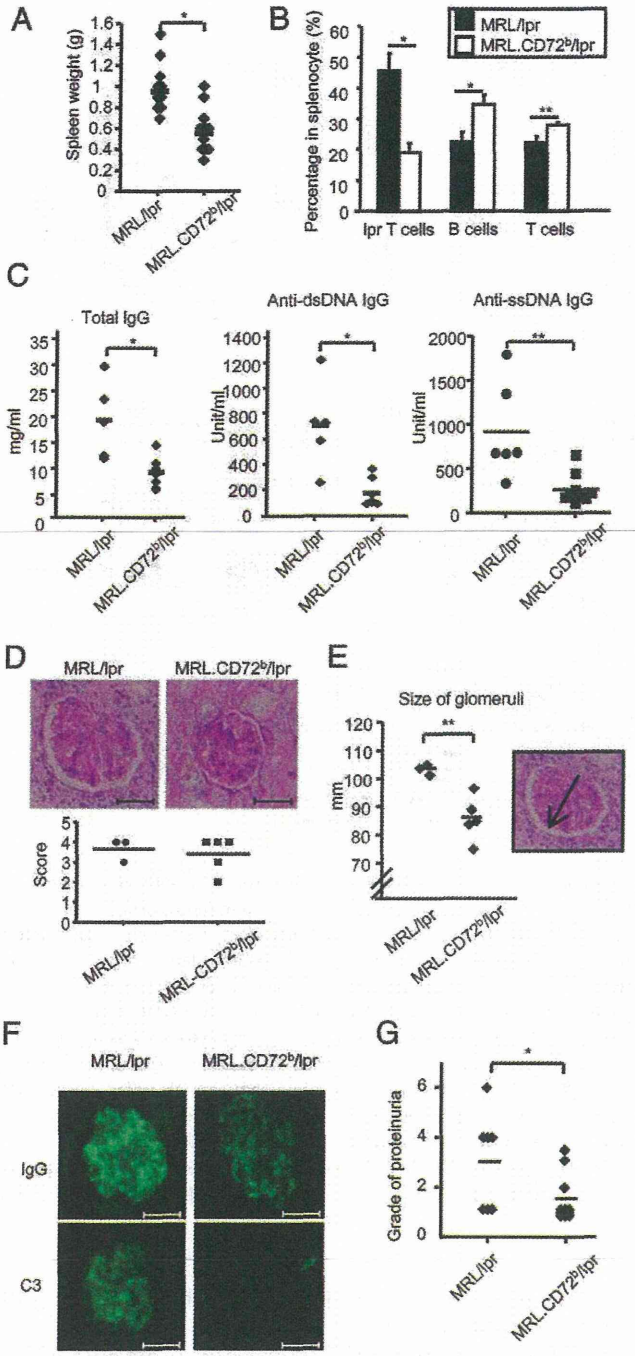

FIGURE 2. Reduced severity of autoimmune disease in MRL.CD72^{b}/lpr mice. Female MRL/lpr and MRL.CD72^{b}/lpr mice at 6 mo old were analyzed. (**A**) Spleen weights (n = 10–16). (**B**) Percentages of lpr T cells (B220^{+}CD3^{+}), B cells (B220^{+}CD3^{-}), and T cells (B220^{-}CD3^{+}) in total lymphocyte-gated splenocytes were measured by flow cytometry (n = 3). (**C**) Concentrations of total IgG and titers of anti-dsDNA and anti-ssDNA IgG in sera were measured by ELISA (n = 5–9). For determining autoantibody titers, pooled sera from >8-mo-old (NZB × NZW) F1 mice are used as a standard (1000 U/ml). (**D**) PASH staining of glomeruli (n = 3–5). Severity of glomerular damage was scored as in the legend to Fig. 1C. Glomeruli are shown at the same magnification. Scale bars, 50 μM. (**E**) Size of glomeruli (n = 3–5). The diameter of glomeruli from vascular pole of five randomly selected glomeruli was measured on PASH-stained sections of kidneys (original magnification ×400). Each dot represents the mean value of the glomerular diameter for each mouse. (**F**) Immunohistochemical analysis of glomeruli for IgG and C3. Representative data of more than three mice in each genotype are shown. Scale bars, 50 μM. (**G**) Urine protein level. Urine was spotted on filter paper, and the protein level was semiquantitatively measured (n = 7–12). The grade of proteinuria was defined as follows: grade 6, equivalent to 30 mg/ml BSA; grade 5, 10 mg/ml BSA; grade 4, 3.3 mg/ml BSA; grade 3, 1.1 mg/ml BSA; grade 2, 0.74 mg/ml BSA; and grade 1, 0.37 mg/ml BSA. *$p < 0.05$, **$p < 0.005$.

genes in the MRL-derived interval in B6.CD72^{c} mice regulate B cell activation is not excluded.

To directly demonstrate that CD72^{c} poorly regulates BCR signaling, we transduced CD72^{c} and CD72^{a}, the latter of which is highly homologous to CD72^{b}, to the mouse B cell line BAL17 and examined their capacity to regulate BCR signaling. As BAL17 cells express endogenous CD72^{b} (34), we examined the expression of the transduced CD72^{a} and CD72^{c} by flow cytometry using anti-CD72 mAbs reactive to CD72^{a} and CD72^{b} and that reactive to CD72^{b} and CD72^{c}, respectively. The expression level of CD72 in BAL17-CD72^{a} transfectant and BAL17-CD72^{c} transfectant are 1.74 and 3.58 times higher than parent BAL17 cells, respectively (Fig. 3D). We are not able to exclude the possibility that these anti-CD72 Abs react to different CD72 allelic forms with different efficiency or the possibility that transduced CD72 affects expression of endogenous CD72 or forms a heterodimer with endogenous CD72. Nonetheless, our result on flow cytometry suggests that CD72^{c} expression in BAL17-CD72^{c} cells is higher than CD72^{a} expression in BAL17-CD72^{a} cells. We then ligated BCR on BAL17 transfectants using anti-IgM Ab and analyzed calcium mobilization and ERK phosphorylation. Both calcium mobilization and ERK phosphorylation induced by BCR ligation were reduced in BAL17-CD72^{a} transfectant compared with control transfectant (Fig. 3E, 3F), indicating that CD72^{a} negatively regulates BCR signaling in agreement with previous findings (14). In contrast, CD72^{c} expression reduced both calcium mobilization and ERK phosphorylation only marginally if any (Fig. 3E, 3F), although the CD72 expression level in CD72^{c} transfectant is higher than that in CD72^{a} transfectant. Thus, CD72^{c} regulates BCR signaling less efficiently than CD72^{a} in both primary B cells and BAL17 cells.

CD72^{c} differs from CD72^{a} or CD72^{b} at the extracellular part but not the cytoplasmic region including ITIM. To address how the extracellular part of CD72^{c} reduces its negative-regulatory activity on B cell activation, we examined association of CD72 to BCR. When we immunoprecipitated CD72^{b} and CD72^{c} from lysates of B6 and B6.CD72^{c} B cells, respectively, CD72^{b} coprecipitated more IgM than CD72^{c} did (Fig. 3G). This result suggests that CD72^{c} associates with BCR less strongly than CD72^{b} does, although we are not able to exclude the possibility that anti-CD72 Abs differently react to the different CD72 allelic forms, resulting in different immunoprecipitation and detection efficiency depending on the allelic forms. Taken together, CD72^{c} regulates B cell signaling and B cell activation inefficiently probably due to its weak association to BCR.

CD72 deficiency causes severe autoimmune disease in the presence of Fas^{lpr} mutation

As CD72^{c} regulates BCR signaling less efficiently than CD72^{a}, we next addressed whether CD72 deficiency induces severe autoimmune disease in the presence of the *Fas^{lpr}* gene by generating *Cd72$^{-/-}$* mice on a B6 background (Supplemental Fig. 2). When we examined signaling properties of *Cd72$^{-/-}$* B6 B cells, BCR ligation–induced ERK phosphorylation was augmented compared with that in wild-type B6 B cells expressing CD72^{b} (Fig. 4A), whereas calcium signaling in *Cd72$^{-/-}$* B cells was similar to that

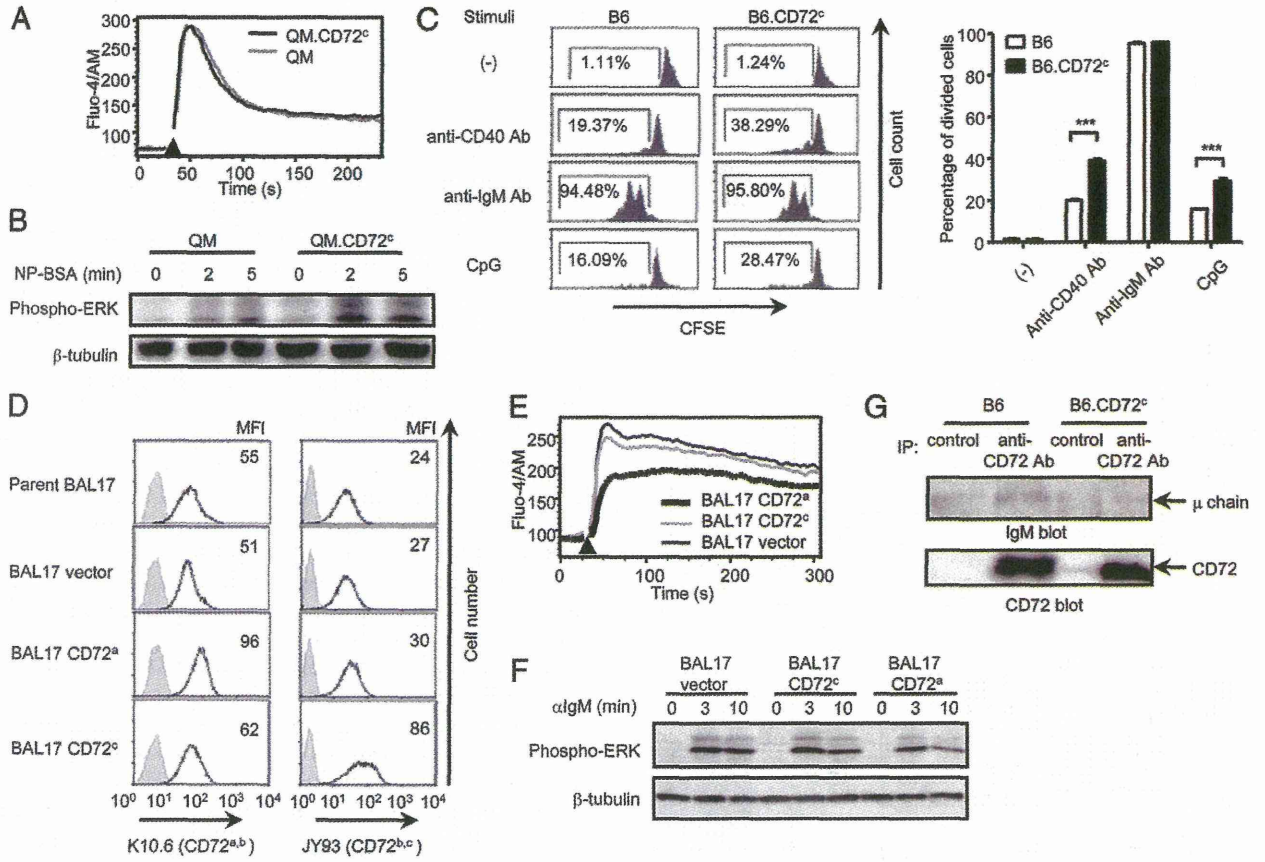

FIGURE 3. CD72^c is a poor negative regulator of BCR signaling and B cell activation. Spleen B cells were purified from 8–12-wk-old QM and QM.CD72^c mice. Fluo-4/AM-loaded (**A**) or untreated (**B**) cells were stimulated with 0.2 μg/ml NP-BSA. Intracellular free calcium ion level was measured by flow cytometry (A). The arrowhead indicates the time point when NP-BSA was added. Alternatively, total cell lysates were analyzed for phosphorylation of ERK by Western blotting (B). The same membrane was reprobed with anti–β-tubulin Ab to ensure equal loading. Representative data of three experiments are shown. (**C**) Purified spleen B cells from B6 or B6.CD72^c mice were labeled with CFSE and cultured with indicated reagents for 72 h. CFSE fluorescence was analyzed by flow cytometry. The percentages of proliferated cells are indicated (*left panel*). Mean ± SD of triplicate is shown (*right panel*). Data are representative of three independent experiments. (**D**) CD72 expression in indicated BAL17 transfectants were analyzed by flow cytometry using anti-CD72 Abs K10.6 reactive to CD72^a and CD72^b and JY/93 reactive to CD72^b and CD72^c. Mean fluorescence intensity (MFI) is indicated. Unstained cells were used as negative controls (shaded histograms). Fluo-4/AM–loaded (**E**) or untreated (**F**) BAL17 transfectants were stimulated with 10 μg/ml anti-IgM Ab. Calcium ion concentration was analyzed by flow cytometry (E). The arrowhead indicates the time point when anti-IgM Ab was added. Representative data of five experiments are shown. Total cell lysates were analyzed for phosphorylation of ERK by Western blotting (F). The same membrane was reprobed with anti–β-tubulin Ab to ensure equal loading. Representative data of three experiments are shown. (**G**) Total cell lysates of purified spleen B cells from B6 and B6.CD72^c mice were immunoprecipitated (IP) with anti-CD72 or control Ab and analyzed by Western blotting using anti-IgM and anti-CD72 Abs. Representative data of three experiments are shown. ***$p < 0.001$.

in wild-type B6 B cells (Fig. 4B). Thus, CD72 appears to efficiently regulate BCR ligation–induced ERK phosphorylation but not calcium signaling in agreement with our results in QM.CD72^c B cells and BAL17 transfectants (Fig. 3). Proliferative response to CpG and anti-CD40 Ab was augmented in *Cd72*$^{-/-}$ B cells compared with wild-type B6 B cells (Fig. 4*C*), as is the case for B6.CD72^c B cells. Thus, signaling and proliferative properties of *Cd72*$^{-/-}$ B cells are similar to those of *Cd72*^{c}-carrying B cells.

We then bred *Cd72*$^{-/-}$ mice with B6/lpr mice and analyzed 6-mo-old female *Cd72*$^{-/-}$ B6/lpr mice. These mice showed severe splenomegaly (Fig. 4D) and lymphadenopathy (data not shown) and marked expansion of lpr T cells in spleen, LNs, and peritoneal cavity (peritoneal exudate cells [PEC]) (Tables II, III), whereas expansion of lpr T cells is mild in B6/lpr mice. As is the case for B6.CD72^c/lpr mice, percentages of T cells and B cells were increased and decreased, respectively, in *Cd72*$^{-/-}$ B6/lpr mice (Table II). In contrast, *Cd72*$^{-/-}$ mice showed mild splenomegaly but no distorted proportions of T and B cells. Thus, CD72 deficiency induces marked splenomegaly synergistically with the *Fas*^{lpr} gene and accelerates expansion of lpr T cells.

Although the serum IgG level in *Cd72*$^{-/-}$ B6 and *Cd72*$^{-/-}$ B6/lpr mice at 6 mo of age were comparable to that in age-matched *Cd72*$^{+/+}$ B6 mice, the high titer of anti-chromatin IgG was produced in both *Cd72*$^{-/-}$ and *Cd72*$^{-/-}$ B6/lpr mice (Fig. 4E). Although the titers of anti-dsDNA and anti-ssDNA IgG were significantly increased in *Cd72*$^{-/-}$ B6 mice compared with *Cd72*$^{+/+}$ B6 mice, the titers of these autoantibodies were markedly higher in *Cd72*$^{-/-}$ B6/lpr mice than in *Cd72*$^{-/-}$ B6 mice (Fig. 4E), suggesting that CD72 deficiency induces production of a large amount of anti-DNA Abs in the presence of the *Fas*^{lpr} gene. Histopathological analysis revealed development of glomerulonephritis with immune complex deposition (Fig. 4F, 4G) and cell infiltration in lung (Fig. 4H) in *Cd72*$^{-/-}$ B6 mice, which are consistent with the previous report (35). *Cd72*$^{-/-}$ B6/lpr mice developed more severe glomerulonephritis and cell infiltration in lung and liver than *Cd72*$^{-/-}$ B6 or B6/lpr mice, suggesting that CD72 deficiency induces development of autoimmune glomeru-

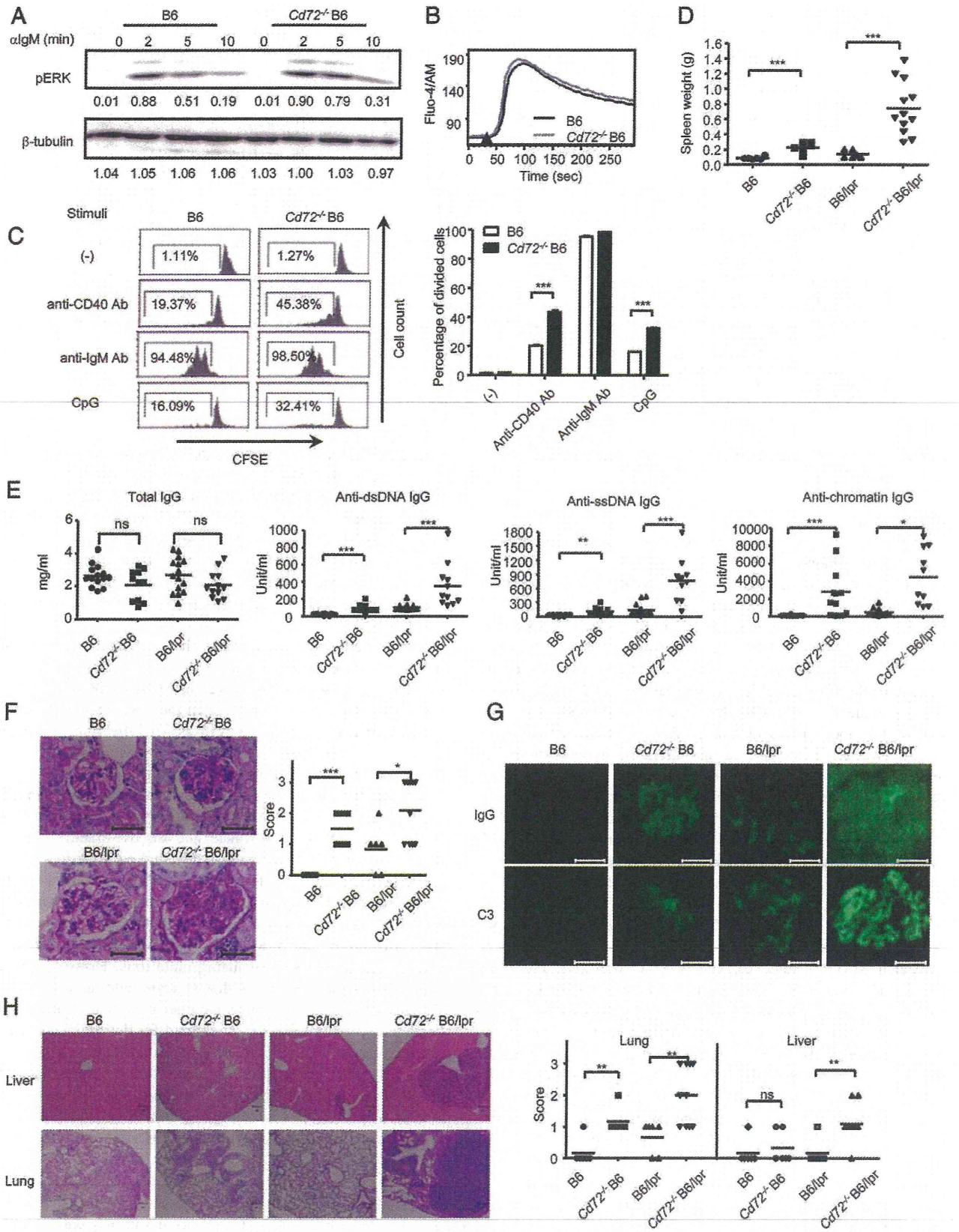

FIGURE 4. Severe autoimmune disease in *Cd72*$^{-/-}$ B6/lpr mice. (**A** and **B**) Spleen B cells were purified from 8–12-wk-old B6 and *Cd72*$^{-/-}$ B6 mice. Total cell lysates were analyzed for phosphorylation of ERK by Western blotting (A). The same membrane was reprobed with anti–β-tubulin Ab to ensure equal loading. The intensity of the protein bands was quantified, and the relative amounts of phosphorylated ERK and β-tubulin are indicated. Representative data of three experiments are shown. Alternatively, Fluo-4/AM–loaded cells were stimulated with 10 μg/ml anti-IgM Ab (B). Intracellular free calcium ion level was measured by flow cytometry. The arrowhead indicates the time point when anti-IgM Ab was added. (**C**) Purified B cells from B6 and *Cd72*$^{-/-}$ B6 mice were labeled with CFSE and cultured with indicated reagents for 72 h. CFSE fluorescence was analyzed by (*Figure legend continues*)

Table II. Flow cytometry analysis of spleen cells from B6, *Cd72*$^{-/-}$ B6, B6/lpr, and *Cd72*$^{-/-}$ B6/lpr mice

Cell Population	B6	*Cd72*$^{-/-}$ B6	B6/lpr	*Cd72*$^{-/-}$ B6/lpr
Total cell number ($\times 10^6$)	98.8 ± 9.3	160.2 ± 15.4	121.6 ± 12.4	308.8 ± 92.8
Phenotype (%)[a]				
B220$^+$CD3$^-$ (B cells)	45.6 ± 2.2	40.0 ± 2.4	55.1 ± 1.3	21.6 ± 3.6**
($\times 10^6$)[b]	(44.5 ± 3.9)	(63.2 ± 6.2)	(66.9 ± 6.5)	(54.4 ± 6.6)
CD3$^+$B220$^-$ (T cells)	41.4 ± 2.7	41.7 ± 1.2	19.4 ± 1.2	31.0 ± 4.2*
($\times 10^6$)	(41.3 ± 5.3)	(66.3 ± 5.6)	(23.8 ± 3.6)	(108.7 ± 49.6)*
B220$^-$CD3$^-$	12.1 ± 1.4	16.3 ± 2.4	8.0 ± 1.0	16.0 ± 2.5*
($\times 10^6$)	(12.0 ± 1.6)	(27.3 ± 5.5)	(9.6 ± 1.2)	(41.9 ± 4.9)**
B220$^+$CD3$^+$ (lpr T cells)	0.9 ± 0.1	2.0 ± 0.5	17.5 ± 1.2	31.3 ± 3.7**
($\times 10^6$)	(0.9 ± 0.2)	(3.4 ± 1.0)	(21.3 ± 2.6)	(103.8 ± 40.5)*
Phenotype of B220$^+$ B cells (%)[b]				
CD21$^{\pm}$CD23^{hi} (FO B cells)	76.1 ± 2.1	52.6 ± 3.1*	46.3 ± 1.4	15.8 ± 5.0***
CD21^{hi}CD23$^{\pm}$ (MZ B cells)	11.0 ± 0.9	7.2 ± 0.7*	10.8 ± 0.9	0.6 ± 0.3***

Data were obtained from 6-mo-old mice and are expressed as mean ± SEM (n = 5 to 6). Statistical significance was calculated between B6 and *Cd72*$^{-/-}$ B6 mice and between B6/lpr and *Cd72*$^{-/-}$ B6/lpr mice.

[a]Percentages of cells expressing the indicated surface markers in lymphocyte-gated cells.

[b]Absolute cell numbers are indicated in parentheses.

*$p < 0.05$, **$p < 0.01$, ***$p < 0.001$.

FO, Follicular; MZ, marginal zone.

lonephritis and cell infiltration in lung and liver synergistically with the *Fas*^{lpr} gene.

Discussion

Autoimmune disease caused by *Fas*^{lpr} depends on the genetic background of mouse strains. In this study, we demonstrate that introduction of the MRL-derived chromosomal interval containing *Cd72*^{c} into B6 mice did not cause any disease but markedly enhanced severity of autoimmune disease in B6/lpr mice. This result clearly demonstrates that this locus contains a modifier gene that regulates *Fas*^{lpr}-induced autoimmune disease. Conversely, introduction of the B6-derived interval containing *Cd72*^{b} reduced the severity of the disease in MRL/lpr mice further support the crucial role of this locus in regulation of *Fas*^{lpr}-induced autoimmune disease. We also demonstrated that CD72^c is hypofunctional in regulating BCR signaling and B cell activation and that CD72 deficiency induces severe autoimmune disease in the presence of *Fas*^{lpr}. Thus, in B6.CD72^c/lpr mice, the hypofunctional *Cd72*^{c} allele but not other genes in the MRL-derived chromosomal interval appears to be responsible for induction of severe autoimmune disease, and *Cd72*^{c} is a modifier gene that regulates *Fas*^{lpr}-induced autoimmune disease.

Our finding on the role of *Cd72*^{c} in development of autoimmune disease is also supported by the finding by Oishi et al. (36). They generated MRL/lpr mice carrying a BAC transgene encoding *Cd72*^{b} and a mutant BAC in which exon 8 encoding a part of the extracellular region of *Cd72* was replaced by the exon 8 derived from *Cd72*^{c}. The *Cd72*^{b}-containing BAC but not the mutant BAC markedly reduced BCR signaling and severity of the autoimmune disease in MRL/lpr mice, clearly demonstrating distinct functional activity of CD72^c and its role in development of autoimmune disease in MRL/lpr mice, in agreement with our finding. Previously, Li et al. (35) demonstrated that *Cd72*$^{-/-}$ mice spontaneously develop autoimmune manifestations including glomerulonephritis and inflammatory infiltration of the lung and salivary glands at 1 y of age, and we confirmed this finding in the independently established *Cd72*$^{-/-}$ mouse line (Fig. 4). Thus, CD72 deficiency but not *Cd72*^{c} causes mild lupus-like disease by itself. *Cd72*^{c} may not cause autoimmune disease by itself as it probably retains its regulatory activity to some extent. Thus, a hypofunctional allele of a gene that is crucial for preventing autoimmune disease can play a role as a modifier gene.

An old study demonstrated that the *Fas*^{lpr} locus induces autoimmune disease in mice with AKR but not C3H or B6 backgrounds (8). Because AKR as well as MRL carries *Cd72*^{c}, *Cd72*^{c} may be a modifier gene involved in the development of autoimmune disease in AKR/lpr as well as MRL/lpr mice. In human, mutations of *Fas* cause autoimmune lymphoproliferative syndrome (ALPS), in which penetrance is variable among families (6, 7, 37). As there is a functional difference between human *CD72* haplotypes (38, 39), CD72 polymorphism may play a crucial role in the regulation of penetrance and disease manifestations in ALPS. Modifier genes are extensively studied in various diseases including cystic fibrosis, arrhythmia, and cancer because modifier genes extensively regulate penetrance, severity, and manifestations of these diseases (1–3). Also, modifier genes can be a good target of therapy and prevention if it is difficult to correct the defect caused by disease-causing mutations. However, little is known about modifier genes that regulate autoimmune diseases. The *Yaa* gene may be another modifier gene that regulates autoimmune diseases because it is required for development of autoimmune disease in BXSB mice but does not induce autoimmune disease by itself in the B6 background (40), although *Yaa* is naturally found only in BXSB mice. As most cases of autoimmune diseases appear to involve multiple genes, all of which contribute to a minor component (41), it may not be straightforward to dis-

flow cytometry. The percentages of proliferated cells are indicated (*left panel*). Mean ± SD of triplicate is shown (*right panel*). Data are representative of three independent experiments. ***$p < 0.0001$. (**D–H**) Female wild-type B6, *Cd72*$^{-/-}$ B6, B6/lpr, and *Cd72*$^{-/-}$ B6/lpr mice at 6 mo old were analyzed. (D) Spleen weight (n = 6–12). (E) Concentrations of total IgG and titers of anti-dsDNA, anti-ssDNA, and anti-chromatin IgG in sera were determined by ELISA. For determining autoantibody titers, pooled sera from >8-mo-old (NZB × NZW) F1 mice are used as a standard (1000 U/ml). Horizontal bars represent mean values (n = 10–14). (F) PASH staining of glomeruli. Severity of glomerular damage was scored as in the legend to Fig. 1C. Scale bars, 50 μM. (G) Immunohistochemical analyses for IgG and C3 in glomeruli. Scale bars, 50 μM. (H) H&E staining of liver and lung (original magnification ×100). Severity of the disease was scored as in the legend to Fig. 1E. Representative data of more than six mice in each genotype are shown. *$p < 0.05$, **$p < 0.005$, ***$p < 0.001$.

Table III. Flow cytometric analysis of LN, bone marrow, and PEC from B6, *Cd72*$^{-/-}$ B6, B6/lpr, and *Cd72*$^{-/-}$ B6/lpr mice

Tissue	Cell Population	B6	*Cd72*$^{-/-}$ B6	B6/lpr	*Cd72*$^{-/-}$ B6/lpr
LN	B220^{+}CD3^{-} (B cells)	28.0 ± 2.1	29.2 ± 2.2	42.2 ± 3.6	13.6 ± 4.2**
	CD3^{+}B220^{-} (T cells)	69.3 ± 2.2	64.8 ± 2.0	10.9 ± 1.0	26.1 ± 2.8**
	B220^{+}CD3^{+} (lpr T cells)	0.4 ± 0.1	0.6 ± 0.1	42.0 ± 4.3	57.7 ± 2.2*
BM	B220^{+}IgM^{-} (pre-B cells)	10.8 ± 1.1	19.5 ± 2.2*	15.4 ± 2.5	8.3 ± 1.6*
	B220^{low}IgM^{low} (immature B cells)	6.5 ± 0.8	6.6 ± 0.3	5.0 ± 0.7	2.2 ± 0.4*
	B220^{+}IgM^{high} (transitional B cells)	2.7 ± 0.5	1.5 ± 0.3	1.8 ± 0.3	0.7 ± 0.4*
	B220^{high}IgM^{low} (mature B cells)	6.5 ± 0.8	4.9 ± 0.6	3.4 ± 1.2	2.6 ± 0.6
PEC	IgM^{high}CD5^{+} (B1-a cells)	12.2 ± 2.9	11.6 ± 3.8	3.1 ± 0.2	4.5 ± 0.1
	IgM^{-}B220^{+}CD5^{+} (lpr T cells)	ND	ND	32.9 ± 6.6	56.0 ± 0.7*

Data were obtained from 6-mo-old mice and are expressed as mean ± SEM (n = 5 to 6). Values represent the percentages of cells expressing the indicated surface makers in total lymphocyte-gated cells from bone marrow (BM), PEC, and LN. Statistical significance was calculated between B6 and *Cd72*$^{-/-}$ B6 mice and between B6/lpr and *Cd72*$^{-/-}$ B6/lpr mice.

*$p < 0.05$, **$p < 0.001$.

ND, Not detected.

tinguish modifier genes from disease-causing genes in autoimmune diseases, except for the cases in which a single gene plays a dominant role, such as patients with ALPS and MRL/lpr mice.

In this study, the autoimmune disease in B6.CD72^{c}/lpr mice is less severe than that in MRL/lpr mice, indicating involvement of other MRL-derived genes in development of the severe disease. This is consistent with the previous findings on the association of other genetic loci such as the *Opn* (20) and *FcγRIIB* loci (42, 43) with development of autoimmune disease in MRL/lpr mice. Thus, multiple genes including *Fas*^{lpr} and *Cd72*^{c} are involved in development of severe autoimmune disease in MRL/lpr mice. Lack of these genes other than *Fas*^{lpr} and *Cd72*^{c} may explain why AKR/lpr develops milder autoimmune disease than MRL/lpr does. Identification of the modifier genes in the MRL background that are involved in the autoimmune disease enables us to study how these genes interact with each other and ultimately induce the autoimmune disease.

It is already well established that CD72 is a negative regulator of BCR signaling (12–16). Expression of CD72^{a} negatively regulates both calcium signaling and ERK phosphorylation induced by BCR ligation in BAL17 cells (Fig. 3). In contrast, *Cd72*$^{-/-}$ B cells show augmented ERK phosphorylation but no alteration in calcium signaling induced by treatment with anti-IgM Ab (Fig. 4A, 4B). However, a previous study demonstrated that BCR ligation-induced calcium response is enhanced in *Cd72*$^{-/-}$ B cells (15, 16). Thus, CD72-mediated regulation of BCR signaling depends on experimental conditions. In the current study, we demonstrated that CD72^{c} is hypofunctional. This property of CD72^{c} may cause enhanced B cell activation, which may be involved in development of autoimmune disease through augmented autoantibody production. The hypofunctional property of CD72^{c} may not be due to its expression efficiency on the cell surface as surface expression level of CD72^{c} in B6.CD72^{c} B cells appears to be equivalent to that of CD72^{b} in B6 B cells, although it is not proven if the anti-CD72 Ab used for measuring CD72 expression level detects CD72^{b} and CD72^{c} equally (Supplemental Fig. 3). In contrast, CD72^{c} coprecipitates BCR less efficiently than CD72^{a} (Fig. 3G), suggesting that interaction of CD72^{c} with BCR is weaker than that of CD72^{a}. As interaction and colocalization of inhibitory coreceptors including FcγRIIB with BCR is crucial for their inhibitory activity (44, 45), less efficient interaction of CD72^{c} with BCR may reduce its regulatory activity on BCR signaling. CD72^{c} contains several amino acid substitutions and a 7-aa deletion in the extracellular region compared with CD72^{a} or CD72^{b}, whereas the cytoplasmic region of CD72^{c} is identical to that of CD72^{a} or CD72^{b} (18, 19). Alterations in the extracellular region of CD72 may change its association with BCR or binding to its ligands, leading to reduction in its colocalization with BCR either directly or indirectly. Although CD100 was reported to be a ligand of CD72 (46), there might be other ligands. Thus, full elucidation of the interaction of CD72 with BCR and ligands may be crucial to understand the defect in signaling function of CD72^{c} and its role in development of autoimmune disease.

Acknowledgments

We thank Dr. T. Kitamura (University of Tokyo, Tokyo, Japan) for cell lines, Dr. M. Wabl (University of California, San Francisco) for QM mice, Dr. N. Tada (Tokai University, Tokyo, Japan) for reagent, Dr. M. Nose (Ehime University, Ehime Prefecture, Japan) for discussion, T. Usami (Tokyo Medical and Dental University) for technical assistance, and S.S. Devi for initial work on the generation of B6.CD72^{c} mice.

Disclosures

The authors have no financial conflicts of interest.

References

1. Cutting, G. R. 2005. Modifier genetics: cystic fibrosis. *Annu. Rev. Genomics Hum. Genet.* 6: 237–260.
2. Nadeau, J. H. 2001. Modifier genes in mice and humans. *Nat. Rev. Genet.* 2: 165–174.
3. Hamilton, B. A., and B. D. Yu. 2012. Modifier genes and the plasticity of genetic networks in mice. *PLoS Genet.* 8: e1002644.
4. Nagata, S. 1998. Human autoimmune lymphoproliferative syndrome, a defect in the apoptosis-inducing Fas receptor: a lesson from the mouse model. *J. Hum. Genet.* 43: 2–8.
5. Watanabe-Fukunaga, R., C. I. Brannan, N. G. Copeland, N. A. Jenkins, and S. Nagata. 1992. Lymphoproliferation disorder in mice explained by defects in Fas antigen that mediates apoptosis. *Nature* 356: 314–317.
6. Rieux-Laucat, F., F. Le Deist, C. Hivroz, I. A. Roberts, K. M. Debatin, A. Fischer, and J. P. de Villartay. 1995. Mutations in Fas associated with human lymphoproliferative syndrome and autoimmunity. *Science* 268: 1347–1349.
7. Fisher, G. H., F. J. Rosenberg, S. E. Straus, J. K. Dale, L. A. Middleton, A. Y. Lin, W. Strober, M. J. Lenardo, and J. M. Puck. 1995. Dominant interfering Fas gene mutations impair apoptosis in a human autoimmune lymphoproliferative syndrome. *Cell* 81: 935–946.
8. Kelley, V. E., and J. B. Roths. 1985. Interaction of mutant lpr gene with background strain influences renal disease. *Clin. Immunol. Immunopathol.* 37: 220–229.
9. Izui, S., V. E. Kelley, K. Masuda, H. Yoshida, J. B. Roths, and E. D. Murphy. 1984. Induction of various autoantibodies by mutant gene lpr in several strains of mice. *J. Immunol.* 133: 227–233.
10. Takahashi, S., S. Futatsugi-Yumikura, A. Fukuoka, T. Yoshimoto, K. Nakanishi, and S. Yonehara. 2013. Fas deficiency in mice with the Balb/c background induces blepharitis with allergic inflammation and hyper-IgE production in conjunction with severe autoimmune disease. *Int. Immunol.* DOI: 10.1093/intimm/dxs109.
11. Nakayama, E., I. von Hoegen, and J. R. Parnes. 1989. Sequence of the Lyb-2 B-cell differentiation antigen defines a gene superfamily of receptors with inverted membrane orientation. *Proc. Natl. Acad. Sci. USA* 86: 1352–1356.
12. Adachi, T., H. Flaswinkel, H. Yakura, M. Reth, and T. Tsubata. 1998. The B cell surface protein CD72 recruits the tyrosine phosphatase SHP-1 upon tyrosine phosphorylation. *J. Immunol.* 160: 4662–4665.
13. Wu, Y., M. J. Nadler, L. A. Brennan, G. D. Gish, J. F. Timms, N. Fusaki, J. Jongstra-Bilen, N. Tada, T. Pawson, J. Wither, et al. 1998. The B-cell trans-

membrane protein CD72 binds to and is an in vivo substrate of the protein tyrosine phosphatase SHP-1. *Curr. Biol.* 8: 1009–1017.
14. Adachi, T., C. Wakabayashi, T. Nakayama, H. Yakura, and T. Tsubata. 2000. CD72 negatively regulates signaling through the antigen receptor of B cells. *J. Immunol.* 164: 1223–1229.
15. Li, D. H., J. W. Tung, I. H. Tarner, A. L. Snow, T. Yukinari, R. Ngernmaneepothong, O. M. Martinez, and J. R. Parnes. 2006. CD72 downmodulates BCR-induced signal transduction and diminishes survival in primary mature B lymphocytes. *J. Immunol.* 176: 5321–5328.
16. Pan, C., N. Baumgarth, and J. R. Parnes. 1999. CD72-deficient mice reveal nonredundant roles of CD72 in B cell development and activation. *Immunity* 11: 495–506.
17. Tung, J. S., F. W. Shen, V. LaRegina, and E. A. Boyse. 1986. Antigenic complexity and protein-structural polymorphism in the Lyb-2 system. *Immunogenetics* 23: 208–210.
18. Robinson, W. H., H. Ying, M. C. Miceli, and J. R. Parnes. 1992. Extensive polymorphism in the extracellular domain of the mouse B cell differentiation antigen Lyb-2/CD72. *J. Immunol.* 149: 880–886.
19. Ying, H., E. Nakayama, W. H. Robinson, and J. R. Parnes. 1995. Structure of the mouse CD72 (Lyb-2) gene and its alternatively spliced transcripts. [Published erratum appears in 1995 *J. Immunol.* 155: 1637b.] *J. Immunol.* 154: 2743–2752.
20. Miyazaki, T., M. Ono, W. M. Qu, M. C. Zhang, S. Mori, S. Nakatsuru, Y. Nakamura, T. Sawasaki, Y. Endo, and M. Nose. 2005. Implication of allelic polymorphism of osteopontin in the development of lupus nephritis in MRL/lpr mice. *Eur. J. Immunol.* 35: 1510–1520.
21. Qu, W. M., T. Miyazaki, M. Terada, L. M. Lu, M. Nishihara, A. Yamada, S. Mori, Y. Nakamura, H. Ogasawara, C. Yazawa, et al. 2000. Genetic dissection of vasculitis in MRL/lpr lupus mice: a novel susceptibility locus involving the *CD72*^{c} allele. *Eur. J. Immunol.* 30: 2027–2037.
22. Nose, M. 2011. A polygene network model for the complex pathological phenotypes of collagen disease. *Pathol. Int.* 61: 619–629.
23. Kitamura, T., Y. Koshino, F. Shibata, T. Oki, H. Nakajima, T. Nosaka, and H. Kumagai. 2003. Retrovirus-mediated gene transfer and expression cloning: powerful tools in functional genomics. *Exp. Hematol.* 31: 1007–1014.
24. Onishi, M., S. Kinoshita, Y. Morikawa, A. Shibuya, J. Phillips, L. L. Lanier, D. M. Gorman, G. P. Nolan, A. Miyajima, and T. Kitamura. 1996. Applications of retrovirus-mediated expression cloning. *Exp. Hematol.* 24: 324–329.
25. Cascalho, M., A. Ma, S. Lee, L. Masat, and M. Wabl. 1996. A quasi-monoclonal mouse. *Science* 272: 1649–1652.
26. Tada, N., S. Kimura, Y. Liu, B. A. Taylor, and U. Hämmerling. 1981. Ly-m19: the Lyb-2 region of mouse chromosome 4 controls a new surface alloantigen. *Immunogenetics* 13: 539–546.
27. Tokushige, K., K. Kinoshita, S. Hirose, and T. Shirai. 1992. Genetic association between natural autoantibody responses to histones and DNA in murine lupus. *Autoimmunity* 12: 285–293.
28. Nomura, T., H. Han, M. C. Howard, H. Yagita, H. Yakura, T. Honjo, and T. Tsubata. 1996. Antigen receptor-mediated B cell death is blocked by signaling via CD72 or treatment with dextran sulfate and is defective in autoimmunity-prone mice. *Int. Immunol.* 8: 867–875.
29. Onodera, T., J. C. Poe, T. F. Tedder, and T. Tsubata. 2008. CD22 regulates time course of both B cell division and antibody response. *J. Immunol.* 180: 907–913.
30. Rolink, A., F. Melchers, and J. Andersson. 1996. The SCID but not the *RAG-2* gene product is required for S μ-S ε heavy chain class switching. *Immunity* 5: 319–330.
31. Heit, A., K. M. Huster, F. Schmitz, M. Schiemann, D. H. Busch, and H. Wagner. 2004. CpG-DNA aided cross-priming by cross-presenting B cells. *J. Immunol.* 172: 1501–1507.
32. Napirei, M., H. Karsunky, B. Zevnik, H. Stephan, H. G. Mannherz, and T. Möröy. 2000. Features of systemic lupus erythematosus in Dnase1-deficient mice. *Nat. Genet.* 25: 177–181.
33. Knight, J. G., D. D. Adams, and H. D. Purves. 1977. The genetic contribution of the NZB mouse to the renal disease of the NZB x NZW hybrid. *Clin. Exp. Immunol.* 28: 352–358.
34. Ogimoto, M., G. Ichinowatari, N. Watanabe, N. Tada, K. Mizuno, and H. Yakura. 2004. Impairment of B cell receptor-mediated Ca^{2+} influx, activation of mitogen-activated protein kinases and growth inhibition in CD72-deficient BAL-17 cells. *Int. Immunol.* 16: 971–982.
35. Li, D. H., M. M. Winslow, T. M. Cao, A. H. Chen, C. R. Davis, E. D. Mellins, P. J. Utz, G. R. Crabtree, and J. R. Parnes. 2008. Modulation of peripheral B cell tolerance by CD72 in a murine model. *Arthritis Rheum.* 58: 3192–3204.
36. Oishi, H., T. Tsubaki, T. Miyazaki, M. Ono, M. Nose, and S. Takahashi. 2013. A bacterial artificial chromosome transgene with polymorphic Cd72 inhibits the development of glomerulonephritis and vasculitis in MRL-Faslpr lupus mice. *J. Immunol.* 190: 2129–2137.
37. Hsu, A. P., K. C. Dowdell, J. Davis, J. E. Niemela, S. M. Anderson, P. A. Shaw, V. K. Rao, and J. M. Puck. 2012. Autoimmune lymphoproliferative syndrome due to FAS mutations outside the signal-transducing death domain: molecular mechanisms and clinical penetrance. *Genet. Med.* 14: 81–89.
38. Hitomi, Y., N. Tsuchiya, A. Kawasaki, J. Ohashi, T. Suzuki, C. Kyogoku, T. Fukazawa, S. Bejrachandra, U. Siriboonrit, D. Chandanayingyong, et al. 2004. *CD72* polymorphisms associated with alternative splicing modify susceptibility to human systemic lupus erythematosus through epistatic interaction with *FCGR2B*. *Hum. Mol. Genet.* 13: 2907–2917.
39. Hitomi, Y., T. Adachi, N. Tsuchiya, Z. I. Honda, K. Tokunaga, and T. Tsubata. 2012. Human CD72 splicing isoform responsible for resistance to systemic lupus erythematosus regulates serum immunoglobulin level and is localized in endoplasmic reticulum. *BMC Immunol.* 13: 72.
40. Izui, S., M. Higaki, D. Morrow, and R. Merino. 1988. The Y chromosome from autoimmune BXSB/MpJ mice induces a lupus-like syndrome in (NZW x C57BL/6)F1 male mice, but not in C57BL/6 male mice. *Eur. J. Immunol.* 18: 911–915.
41. Wakeland, E. K., K. Liu, R. R. Graham, and T. W. Behrens. 2001. Delineating the genetic basis of systemic lupus erythematosus. *Immunity* 15: 397–408.
42. Jiang, Y., S. Hirose, M. Abe, R. Sanokawa-Akakura, M. Ohtsuji, X. Mi, N. Li, Y. Xiu, D. Zhang, J. Shirai, et al. 2000. Polymorphisms in IgG Fc receptor IIB regulatory regions associated with autoimmune susceptibility. *Immunogenetics* 51: 429–435.
43. Pritchard, N. R., A. J. Cutler, S. Uribe, S. J. Chadban, B. J. Morley, and K. G. Smith. 2000. Autoimmune-prone mice share a promoter haplotype associated with reduced expression and function of the Fc receptor FcgammaRII. *Curr. Biol.* 10: 227–230.
44. Tsubata, T. 1999. Co-receptors on B lymphocytes. *Curr. Opin. Immunol.* 11: 249–255.
45. Smith, K. G., and M. R. Clatworthy. 2010. FcgammaRIIB in autoimmunity and infection: evolutionary and therapeutic implications. *Nat. Rev. Immunol.* 10: 328–343.
46. Kumanogoh, A., C. Watanabe, I. Lee, X. Wang, W. Shi, H. Araki, H. Hirata, K. Iwahori, J. Uchida, T. Yasui, et al. 2000. Identification of CD72 as a lymphocyte receptor for the class IV semaphorin CD100: a novel mechanism for regulating B cell signaling. *Immunity* 13: 621–631.

RESEARCH ARTICLE

REVISED Excess CD40L does not rescue anti-DNA B cells from clonal anergy [v2; ref status: indexed, http://f1000r.es/2rs]

Mohammad Aslam , Yusuke Kishi, Takeshi Tsubata

Department of Immunology, Medical Research Institute, Tokyo Medical and Dental University, Tokyo, 113-8510, Japan

v2 **First published:** 17 Oct 2013, **2**:218 (doi: 10.12688/f1000research.2-218.v1)
Latest published: 15 Jan 2014, **2**:218 (doi: 10.12688/f1000research.2-218.v2)

Abstract

CD40L, a member of the tumor necrosis factor (TNF) ligand family, is overexpressed in patients with systemic lupus erythematosus and in lupus mouse models. Previously, we demonstrated that B cells producing pathogenic anti-Sm/RNP antibodies are deleted in the splenic marginal zone (MZ), and that MZ deletion of these self-reactive B cells is reversed by excess CD40L, leading to autoantibody production. To address whether excess CD40L also perturbs clonal anergy, another self-tolerance mechanism of B cells whereby B cells are functionally inactivated and excluded from follicles in the peripheral lymphoid tissue, we crossed CD40L-transgenic mice with the anti-DNA H chain transgenic mouse line 3H9, in which Ig λ1+ anti-DNA B cells are anergized. However, the percentage and localization of Ig λ1+ B cells in CD40L/3H9 double transgenic mice were no different from those in 3H9 mice. This result indicates that excess CD40L does not perturb clonal anergy, including follicular exclusion. Thus, MZ deletion is distinct from clonal anergy, and is more liable to tolerance break.

Article Status Summary

Referee Responses

Referees	1	2	3
v1 published 17 Oct 2013	✓ report	? report	✗ report
v2 published 15 Jan 2014 REVISED		✓ report	✓ report

1 **Marko Radic**, University of Tennessee Health Science Center USA

2 **Jennifer Marshall**, University of Birmingham UK

3 **David Nemazee**, Scripps Research Institute USA

Latest Comments

No Comments Yet

Corresponding author: Takeshi Tsubata (tsubata.imm@mri.tmd.ac.jp)

How to cite this article: Aslam M, Kishi Y and Tsubata T (2014) **Excess CD40L does not rescue anti-DNA B cells from clonal anergy [v2; ref status: indexed, http://f1000r.es/2rs]** *F1000Research* 2014, **2**:218 (doi: 10.12688/f1000research.2-218.v2)

Grant information: This work was supported by MEXT KAKENHI Grants Number 23390063 (TT) and 24790464 (YK).
The funders had no role in study design, data collection and analysis, decision to publish, or preparation of the manuscript.

Competing interests: No competing interests were disclosed.

First published: 17 Oct 2013, **2**:218 (doi: 10.12688/f1000research.2-218.v1)
First indexed: 28 Jan 2014, **2**:218 (doi: 10.12688/f1000research.2-218.v2)